We are IntechOpen, the world's leading publisher of Open Access books Built by scientists, for scientists

4,800
Open access books available

122,000
International authors and editors

135M
Downloads

Our authors are among the

154
Countries delivered to

TOP 1%
most cited scientists

12.2%
Contributors from top 500 universities

CLARIVATE ANALYTICS BOOK CITATION INDEX INDEXED

WEB OF SCIENCE™

Selection of our books indexed in the Book Citation Index in Web of Science™ Core Collection (BKCI)

Interested in publishing with us?
Contact book.department@intechopen.com

Numbers displayed above are based on latest data collected.
For more information visit www.intechopen.com

Chapter 2

Spectroscopic and Optoelectronic Properties of Hydrogenated Amorphous Silicon-Chalcogen Alloys

Shawqi Al Dallal

Additional information is available at the end of the chapter

http://dx.doi.org/10.5772/61103

Abstract

Hydrogenated amorphous silicon-chalcogen alloy thin films have been the subject of growing interest during the past two decades. Thin films of these alloys are usually prepared by the decomposition of SiH_4 and H_2S or H_2Se gas mixtures in a radiofrequency plasma glow discharge at a substrate temperature of 250°C. The alloy composition is varied by changing the gas volume ratio R_V = [chalcogen/silane]. Infrared spectroscopy is used to explore the bonding structure of the alloy. The material exhibits hydrogen-induced bands, normally observed in a-Si:H spectra and other chalcogen-induced bands resulting from bonding chalcogen atoms with hydrogen and silicon. Analysis of the vibrational spectra of this material reveals the presence of significant levels of Si-chalcogen-SiH_n configurations. Optical and electrical measurements show that increasing the chalcogen content results in an increase of the optical (Tauc) gap and a decrease in dark conductivity and photoconductivity. Subgap absorption measurements are employed to probe the Urbach energy and defect density. Upon increasing the chalcogen content, a broadening of band tails and an increase in defect density is observed. These results are shown to be consistent with photoluminescence measurements carried out on these materials.

Keywords: Amorphous silicon alloys, Sulphur, Selenium, Infrared spectroscopy, Photoconductivity, Photoluminescence

1. Introduction

There has been an intensive research work during the past two decades to search for stable and low defect density material for use in tandem with a-Si:H-based photovoltaic devices [1–5]. a-Si:H-based alloys proved to be attractive materials with a wide range of applications including solar cells, photoreceptors, displays, and imaging devices [6–9]. Hydrogenated carbon alloys (a-Si, C:H) have received the most interest [10–12]. However, substantial work has been conducted to study alternatives to this material with comparable properties. Nanostructured hydrogenated silicon (ns-Si:H) prepared by plasma-enhanced chemical vapour deposition at 27.12 MHz was found to exhibit a wide range of applications including solar cells, integrated arrays of printed circuit devices [13,14], and thin film transistors [15].

Hydrogenated polymorphous silicon also proved to be a viable alternative material to produce low-cost solar cells [16]. This material is made up of small clusters containing nanocrystals imbedded in the silicon amorphous matrix. This structure is different from traditional hydrogenated amorphous and microcrystalline silicon thin films. It exhibits better electronic properties and is a more optically stable material. No attempt has been made so far to incorporate chalcogen into this material, and this remains an area of potential interest.

a-Si,S:H [17–20] and a-Si,Se:H [21,22] alloys proved to be of particular interest because they exhibit a juxtaposition of chalcogenide and silicon-based semiconductors with a wide range of optical and electronic properties.

In this paper, we provide a review of the preparation, spectroscopic, and optoelectronic characterization of amorphous silicon-chalcogen alloys thin films. Sulphur and selenium are revealed to be among the most appropriate elements to form alloys with silicon of potential applications in optoelectronic devices [23,24]. Addition of sulphur or selenium to the amorphous silicon matrix to form a-Si_x S_{1-x} H or a-Si_x Se_{1-x} H alloys and the possibility of changing the composition gives rise to a wider range of properties of this material. Of particular relevance are the nature and properties of defect states of various compositions and their influence on the optical parameters and charge transport phenomenon. The study of the infrared (i.r.) vibrational spectra and its correlation with the electronic and optical properties of the material reveals interesting information regarding the structure of the alloy and the nature of defect states in the bandgap. The compositional dependence of hydrogenated silicon-chalcogen alloy will be shown to have an important impact on its optical bandgap and transport properties. The glow discharge experimental technique can also be employed to prepare superlattices of a controlled number of layers as revealed by small angle x-ray diffraction technique [25].

2. Experimental

Hydrogenated amorphous silicon-sulphur and silicon-selenium alloy thin films have been prepared by capacitively coupled radiofrequency (rf) glow-discharge decomposition of (5%

http://dx.doi.org/10.5772/61103

SiH_4 + 95% He) and (2% H_2S or H_2Se + 98% He) gas mixtures. Helium dilution of the reactant gases is employed for safety purposes. Handling of H_2S or H_2Se gases requires extreme precautions because of its toxicity and bad smell. Thin films are normally deposited on 7059 Corning glass or on high-resistivity silicon substrates held at 250°C. The plasma power was controlled at 0.4 Torr, whereas the power density was varied between 5 and 50 W. The power density of 20 W plasma power translates to about 110 mW/m^2. For a total flow rate of reactant gases of typically 30 cm^3/min, a growth rate of about 2 Å/s for equal flow rates of silane and hydrogen-chalcogen gas was obtained. The decomposition rate was found to be a function of the gas volume ratio $R_V \equiv$ [chalcogen/silane]. Increasing R_v above a threshold value leads to a rapid decrease in the growth rate.

3. Results and discussion

Infrared transmission measurements on a-$Si_{1-x}S_x$:H and $Si_{1-x}Se_x$:H alloys with different compositions are depicted in Figs. (1) to (6). The spectra of these two alloys will be discussed separately and then compared to elucidate their nature, origin, and bonding environment.

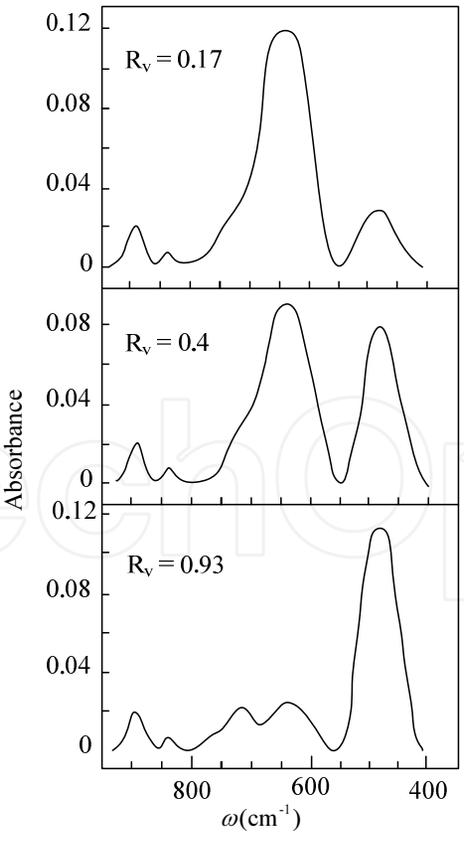

Figure 1. Compositional dependence of the infrared absorption spectra of a-Si,S:H alloy in the range 400–1000 cm^{-1}. Deposition parameters were: T_s = 250°C, P = 0.5 Torr, plasma power = 20 W (Ref. 15).

3.1. Infrared spectra of a-Si_{1-x} S_x:H alloys

Figs. (1) and (2) show the infrared (i.r.) spectra of a-$Si_{1-x}S_x$:H film in the 400–4000 cm^{-1} range. We can distinguish two types of bands in these spectra. The first is the hydrogen-induced band, and covers the spectral range from 500 to 900 cm^{-1} and from 1900 to 2300 cm^{-1}. The second is the sulphur-induced band appearing in the same spectral range. In the following section, we will discuss separately the characteristics and origin of these bands.

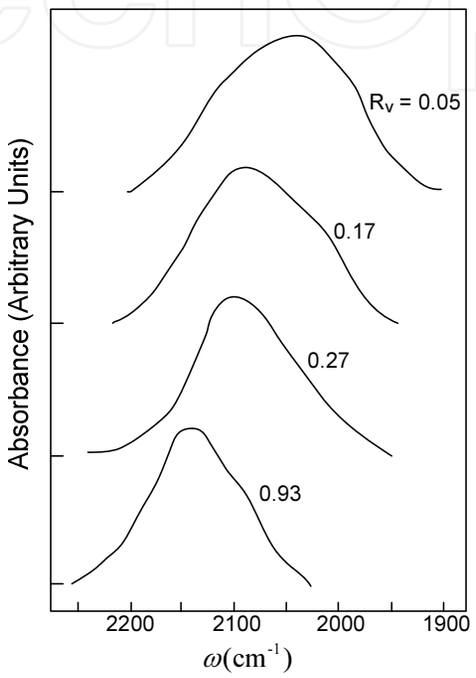

Figure 2. Evolution of the infrared transmission spectra of a-Si,S:H alloys in the 1900–2300 cm^{-1} range with composition. Spectra are normalized to the same maximum intensity. Deposition parameters were: T_s = 250°C, P = 0.5 Torr, plasma power = 20 W (Ref. 15).

3.1.1. Si-H-induced bands in the 500–900 cm^{-1} region

Referring to Fig. (1), the two bands at 840 and 885 cm^{-1} were ascribed by Lucovsky et al. (1979) to the bending modes of SiH_2 bonds. These authors have also demonstrated that isolated dihydrides (SiH_2) appear as a single band at 885 cm^{-1}, whereas polysilane chains give rise to two bands at 890 and 850 cm^{-1}. Because of the relative weakness of the band appearing at 840 cm^{-1} in a-$Si_{1-x}S_x$:H alloy, the band at 885 cm^{-1} was attributed primarily to bending modes of isolated dihydrides [26]. In a-Si:H, the SiH_3 radicals causes a degenerate deformation and symmetric deformation modes at 907 cm^{-1} and 862 cm^{-1} respectively. The absence of these modes in a-Si,S:H alloys' spectra suggests negligible SiH_3 bonding in these alloys [19].

The prominent band at 640 cm^{-1} is dominant in a-Si:H as well as in a-$Si_{1-x}S_x$:H alloys. It was attributed to the wagging mode of Si-H bonds and to the rocking and wagging modes of SiH_2 bonds [27–29].

http://dx.doi.org/10.5772/61103

3.1.2. Stretching mode spectra in the 1900–2300 cm^{-1} region

Figure (2) shows the absorption spectra in the Si-H bond stretching region for different compositions (R_v). This region is normally characterized by the presence of two broad bands at 2000 and 2100 cm^{-1}. These bands are attributed to the Si-H stretching vibrational modes [29]. The stretching mode of Si-H monohydrides appears at 2000 cm^{-1} and that of SiH_2 isolated dihydrides and polysilane chains $(SiH_2)_n$ appears in the region 2090–2100 cm^{-1}. These modes appear in Fig. (2) with a slightly shifted peak position. The mode at 2121–2140 cm^{-1} was assigned to SiH_3 stretching vibrations [26,27].

3.1.3. Sulphur-induced bands in the stretching mode spectral region

Investigation of the stretching region, Fig. (3), shows a systematic shift of the peak position in this region to higher wave numbers as the sulphur content increases. Since the electronegativity of sulphur is larger than that of silicon, this shift was attributed to induction effects induced by sulphur atoms on the Si-H stretching mode frequency in the Si-S-H group, where sulphur and hydrogen are back bonds to the same silicon atom [19]. The frequency of the perturbed Si-H stretching mode can be estimated from the work of Lucovesky [30],

$$\nu\left(S_iH\right) = a + b\sum_{i=1}^{3} SR\left(X_i\right) \tag{1}$$

and

$$\nu\left(S_iH_2\right) = c + d\sum_{i=1}^{2} SR\left(X_i\right) \tag{2}$$

where a, b, c, and d are constants, and $SR(X_i)$ is the electronegativity of the substituted element as defined by Sanderson [31]. For silicon, SR(Si) = 2.62, and for sulphur SR(S) = 4.1 [31]. Using these values and the values of the constants given by Lucovesky, it was found that the substitution of one silicon atom by one sulphur atom in $(Si)_3SiH$ species shifts the Si-H stretching frequency from 2000 cm^{-1} (without sulphur) to 2064 cm^{-1} (with sulphur). For SiH_2 species, the substitution of silicon with sulphur shifts the 2100 cm^{-1} peak to 2127 cm^{-1}, whereas substitution of two silicon atoms with sulphur atoms in the above species shifts the 2000 and the 2100 cm^{-1} bands to 2116 and 2165 cm^{-1}, respectively. The calculated frequencies of these bands were found close to the position of the peak of the stretching band and other pronounced features in a-Si,S:H spectra in this region. It was suggested that the bands in this region are produced by mixing of vibrational modes of SiH, SiH_2, $(Si)_2$ SSiH, $SiSSSiH_2$ and S_2SiH_2 species [19].

3.1.4. Sulphur-induced bands in the 400–500 cm^{-1} region

This region is characterized by a dominant band appearing between 480 and 490 cm^{-1}, as shown in Fig. (1). This band is degenerate with the Si TO-like vibrational mode in amorphous silicon,

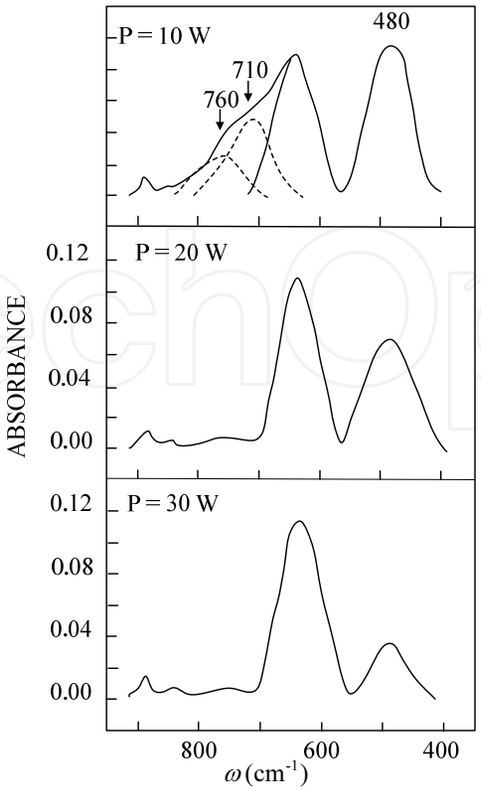

Figure 3. Variation of the infrared absorption spectra of a-SiS:H alloy with r.f. plasma power. For these samples, 10 cm^3 min^{-1} hydrogen flow rate was added to the gaseous mixture. Other deposition parameters were: T_s = 250, P =2 Torr, R_v = 0.6 (Ref. 15).

and is normally i.r. inactive but becomes activated by alloying the Si matrix with an element, such as sulphur, whose elecronegativity is sufficiently different from Si so as to be able to induce charge transfer through the back bonds. In fact, many authors have reported the association of an i.r band with lattice vibrations at 510 cm^{-1} in a-Si,F:H alloys [32,33], and at 500 cm^{-1} in a-Si,Cl:H alloys [34]. Both F and Cl are more electronegative than Si (2.65). This difference in electronegativity is responsible for the shift in the phonon vibrational mode peak to higher wave numbers. Bonding of sulphur atoms to the Si-matrix is also expected to activate the Si-TO-like mode in a-Si,S:H alloys [19]. However, since the electronegativity of S (4.1) is less than that of F or Cl, only a small shift of the phonon band is expected to occur, and the strength of the resulting i.r. band becomes relatively weak.

It was shown that S-S stretching vibrations normally occur as a very weak band in the 400–500 cm^{-1} spectral region [35], and therefore are unlikely to be responsible for the 480–490 cm^{-1} band. Fig. (1) shows that the intensity of this band is appreciably enhanced by increasing the sulphur content in the gas phase. It is therefore believed that bonded sulphur in the form Si-S is responsible for this enhancement [19]. Furthermore, it was found that this band is i.r. and Raman active [36]. Therefore, the 480–490 cm^{-1} band was assigned to the stretching frequencies of the Si-S bonds. In fact, a band near 480 cm^{-1} was first observed by Ebsworth et al. [37] in disilyl sulphide and was attributed to the stretching frequencies of the Si-S bonds.

http://dx.doi.org/10.5772/61103

Of particular interest is the possibility of the presence of SiS_2 species in a-Si,S:H alloys. Studies reported for glassy SiS_2 have shown the existence of three IR active modes at 597, 481, and 395 cm^{-1} [39]. Among the above vibrations, only the 481 cm^{-1} frequency is detected in a-Si,S:H, and therefore, the presence of SiS_2 species in this alloy is unlikely [19].

The effect of plasma power on the i.r. absorption spectra of a-Si,S:H is shown in Fig. (3). An important feature displayed by these spectra is the decrease in the intensity of the 480 cm^{-1} band as the plasma power increases. At low plasma power, a dominating broad band in the 600–800 cm^{-1} region appears. In fact, this region consists of a superposition of several bands, making the analysis more difficult to achieve. However, the broad band can be deconvoluted into three different band at 640, 710, and 760 cm^{-1}, as shown in Fig. (3). The band at 710 cm^{-1} was more pronounced in samples prepared with additional hydrogen flow [19]. Its spectral position is close to the calculated (701 cm^{-1}) and observed (725.8 cm^{-1}) values of the vibrational frequency of the S_2 molecule [39]. Thus, the band at 710 cm^{-1} was assigned tentatively to isolated S_2 molecules trapped in the silicon-sulphur matrix. In fact, the 710 cm^{-1} band is drastically suppressed by increasing the plasma power where the molecule is either dissociated or transferred to the gaseous phase. The band at 760 cm^{-1} is close to the calculated (726 cm^{-1}) and observed (749 cm^{-1}) vibrational frequencies of the SiS molecule [39–41]. However, we think that more experimental data are required to probe the nature of this band. An important aspect of these spectra is the decrease of the 480 cm^{-1} band intensity as the plasma power increases. Figure (4) depicts the variation of the 480 cm^{-1} band intensity with plasma power. It decreases steadily and then levels off at high plasma power. This trend suggests a decrease in the amount of incorporated sulphur atoms with increasing plasma power. This observation is supported by the optical gap measurements which show similar behavior with increasing plasma power.

3.2. Infrared spectra of a-Si,Se:H alloys

Infrared spectroscopy was employed to study the structure of a-Si,Se:H alloys in the 200–4000 cm^{-1} range. Figure (5) depicts the i.r. spectra of a-$Si_{1-x}Se_x$:H alloys in the 200–900 cm^{-1} region. As in the case of a-Si,S:H, the bands at 840 and 885 cm^{-1} are ascribed to the bending modes of SiH_2 bonds [26], whereas the band at 640 cm^{-1} is ascribed to the wagging mode of Si-H bonds and to the rocking and wagging modes of the SiH_2 bonds [27–29]. The band appearing in the region between 480 and 500 cm^{-1} is the Si TO-like phonon mode [27]. The intensity of the band at 390 cm^{-1} was observed to grow with increasing the selenium content in the gas phase. It was first observed by Ebsworth et al. [37] and Tenhover et al. [38] in disilyl selenide and was ascribed to the vibrational mode of the Si-Se bonds. The correlation between R_v in a-Si, Se:H alloys and the intensity of this band is consistent with the above assignment [26].

Figure (6) shows the stretching modes region of a-Si,Se:H alloys. It is dominated by two bands at 2000 and 2100 cm^{-1}, attributed in a-Si:H to the Si-H and SiH_2 configurations, respectively. Incorporation of Se atoms gives rise to the appearance of pronounced features at 2035, 2140, and 2165 cm^{-1}. Referring to the work of Lucovesky discussed in Section 3.1.3, the Si-H stretching mode is affected by the presence of substituted elements of higher electronegativity. Thus, since the electronegativity of Se atoms (4.1) is higher than that of Si (2.65), a shift of the vibrational frequency of the Si-H stretching modes to higher wave number is expected.

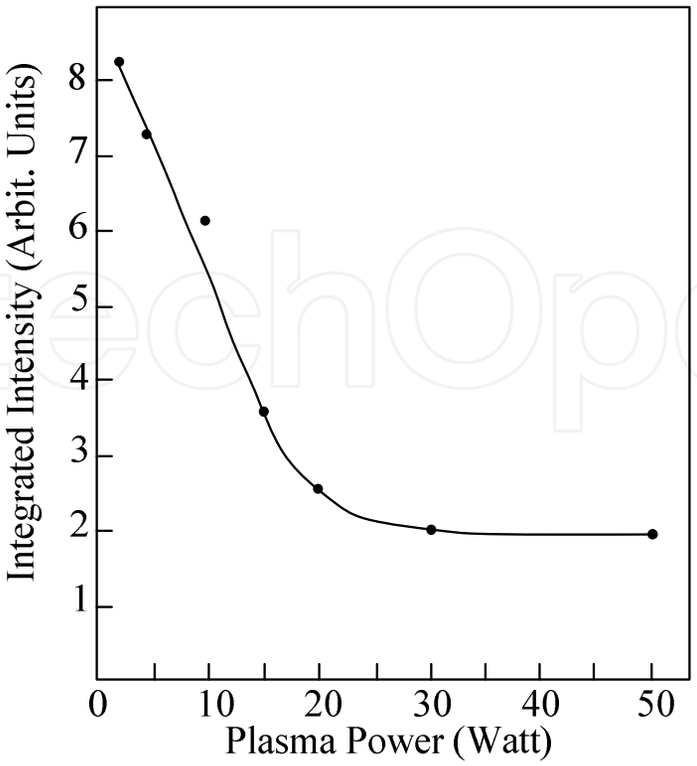

Figure 4. Variation of the integrated intensity of the 480 cm^{-1} band with plasma power (Ref. 15).

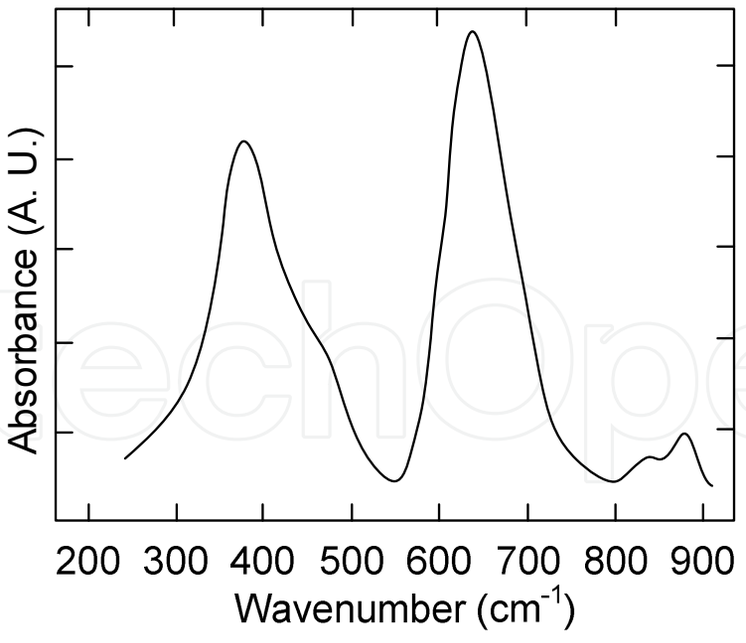

Figure 5. Infrared absorption spectrum of a typical a-Si,Se:H alloy film in the range 250–900 cm^{-1} (Ref. 18).

Analysis of this shift reveals that the bands in the 2000–2100 cm^{-1} region are due to a mixture of the stretching vibrational modes of $(Si)_xSe_{3-x}SiH$ and $(Si)_ySe_{2-y}SiH_2$ species [21].

http://dx.doi.org/10.5772/61103

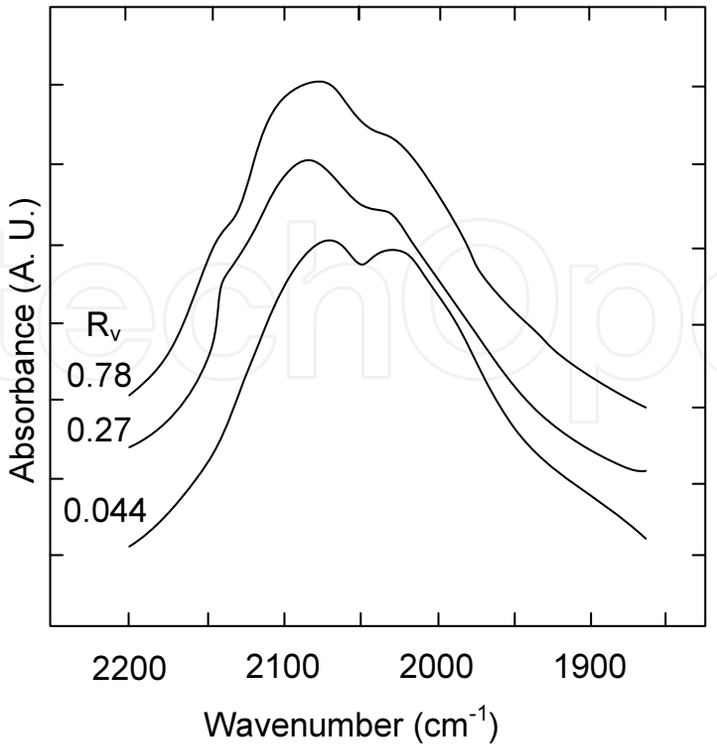

Figure 6. Compositional dependence of the infrared spectra of a-Si,Se:H alloys in the stretching mode region (1800–2200 cm^{-1}) for R_v = 0.44, 0.27, and 0.78 (Ref. 17).

3.3. Optical absorption

The optical (Tauc) gap E_{opt} is determined from optical transmission measurements. Assuming a parabolic density of states for the band tail and an energy independent matrix element for optical transitions between the initial and final states, the absorption coefficient $\alpha(E)$ is given by the relation

$$\alpha h\nu = A\left(h\nu - E_{opt}\right)^2 \tag{3}$$

where A is a constant, and E_{opt} is the optical (Tauc) gap. E_{opt} can be determined by the extrapolation of $(\alpha h \nu)^{1/2}$ towards the base line. This technique proves to be fruitful for measuring E_{opt} for any given sample and was used to determine the compositional dependence of E_{opt} as given in the next section.

3.3.1. Compositional dependence of energy gap in amorphous silicon-chalcogen alloys

The optical (Tauc) gap was measured for samples prepared at different gas volume ratio for both a-Si,S:H and a-Si,Se: alloys, as depicted in Figs. (7) and (8). These figures reveal that the variation of E_{opt} with R_v is not linear. It increases rapidly with the initial introduction of H_2S or H_2Se in the gaseous phase and then levels off at intermediate values of R_v. It increases again

for R_v above 0.6 in a-Si,S:H or R_v above 0.8 in a-Si,Se:H. The E_{opt} dependence on R_v has an inverted s-shaped behavior. The same type of variation was also reported by Saito et al. [42] in a-Si,C:H, indicating that the compositional dependence of E_{opt} is universal in these types of alloys. A model was developed to explore the nature of this variation [43]. The overall compositional dependence of E_{opt} in silicon-sulphur alloys can be derived from Fig. (6) and can be written as

$$y_s = 1.958 - 0.135e^{-x/a_s} + 0.135e^{(x-x_{fs})/b_s} \tag{4}$$

where for a-Si,S:H alloys a_s=0.15, b_s=0.157, and x_{fs}=0.942.

Similarly, the compositional dependence of amorphous silicon-selenium alloy (Fig. 7) can be written as

$$y_{se} = 2.026 - 0.2e^{-x/a_{se}} - e^{(x-x_{fse})/b_{se}} \tag{5}$$

where a_{se}=0.37, b_{se}=0.38, and x_{fse}=2.1.

The significance of the (a) parameter can be evaluated by considering the ratio

$$\frac{a_{se}}{a_s} = 2.467 \tag{6}$$

The above ratio compares closely well with the ratio of the atomic weights of sulphur and selenium

$$\frac{\text{atomic weight of selenium}}{\text{atomic weight of sulphur}} = \frac{78.96}{32.066} = 2.462 \tag{7}$$

To verify the possible bias of the data, the authors [43] applied the same model to a-Si,C:H reported by Saito et al. [42]. The best fit of their data on a-Si,C:H can be approximated by the relation

$$y_C = 1.92 - 0.57\left(e^{-x/0.057} - e^{(x-0.68)/0.08}\right) \tag{8}$$

Thus, a_c=0.057, and

$$\frac{a_c}{a_s} = 0.38 \tag{9}$$

http://dx.doi.org/10.5772/61103

The above relation may be compared with the ratio of the atomic weights of carbon and sulphur

$$\frac{\text{atomic weight of carbon}}{\text{atomic weight of sulphur}} = \frac{12.010}{32.066} = 0.3745 \tag{10}$$

The above ratio is again very close to the predicted value, which provides an extra degree of confidence in the model. This behavior must have a deeper origin at the atomic scale. The atomic weight ratio can be understood by considering processes occurring immediately after the chalcogen atoms are deposited on the film surface. Careful analysis of these processes yield

$$\frac{a_{se}}{a_s} = \frac{\mu_s}{\mu_{se}} = \frac{m_{se}}{m_s} \tag{11}$$

where $\mu = e\tau_{col}/m$ is the mobility of atoms during the diffusion process to occupy their final site, and τ_{col} is the time between successive collisions with the background silicon matrix. Eq. (11) provides a strong hint as to the nature of the processes leading to the observed compositional dependence of the energy gap.

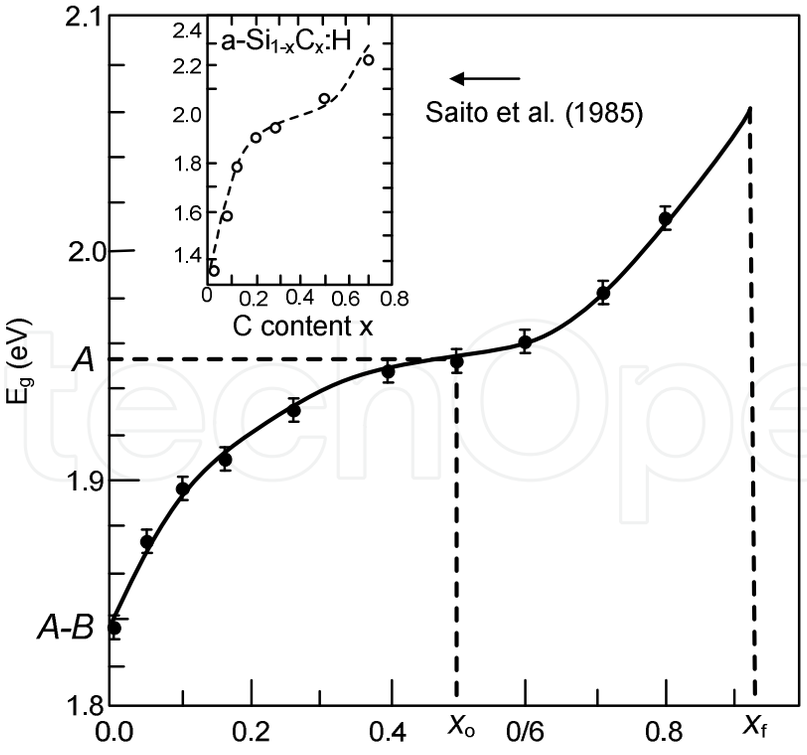

Figure 7. Compositional dependence of the energy (Tauc) gap of a-Si,S:H thin films. A, B, x_o, and x_f are model parameters. The inset shows the compositional dependence of a-Si,C:H reported by Saito et al. [42] (Ref. 17).

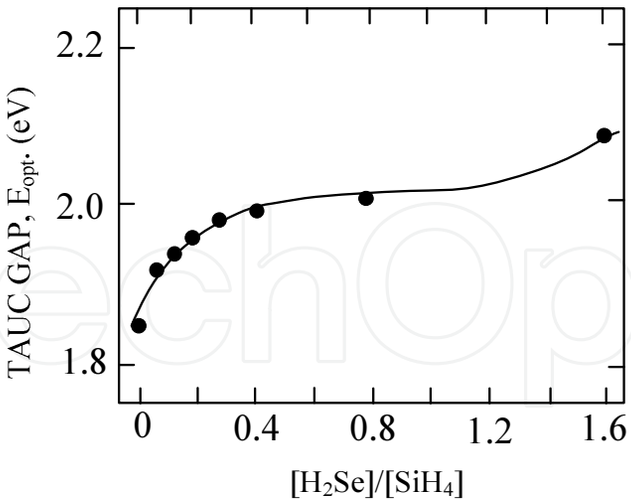

Figure 8. Compositional dependence of the optical (Tauc) gap of a-Si,Se:H (Ref. 17).

3.3.2. Optical subgap absorption, Urbach energy, and defect density

The technique used by employing Eq. (3) proves to be fruitful for determining E_{opt} for given samples, but was found to be limited when probing the structure or deep states in the band tail. For this purpose, other techniques are usually employed, as explained below.

Constant photocurrent method (CPM) is revealed as an accurate approach to measure the optical absorption spectra in the band tail [29]. Below E_{opt}, the spectra exhibits an exponential tail given by

$$\alpha = \alpha_o \exp\left(h\nu / E_u\right) \tag{12}$$

where E_u is the Urbach energy. A plot of the spectra measured for two films of a-Si,Se:H alloys is shown in Fig. (9). The distribution of localized states in the gap was investigated in detail [21,22]. In the following, we shall discuss separately the subgap absorption spectra in amorphous silicon-sulphur and amorphous silicon-selenium alloys respectively.

i. a-Si,S:H alloys: The subgap absorption spectra were measured via constant photocurrent method (CPC) and photothermal deflection spectroscopy (PDS) [22]. The compositional dependence of the Urbach energy E_u and of the defect density N_d are shown in Fig. (10) [22]. E_u rises from 60 to 110 meV as R_v increases from 0 (no sulphur) to 1.1. This variation suggests a substantial increase in the defect density and consequently in the width of the band tails. The increase in N_d is corroborated by the results of ESR measurements of the Si dangling bond spin density N_s. For a-Si,S:H alloys, it was found that N_s increases from 5×10^{16} cm^{-3} in nonalloyed material to about 1×10^{18} cm^{-3} in a 2.2 energy gap material [22]. The alloy also exhibits a substantial LESR signal throughout the entire compositional range, indicating that a substantial

http://dx.doi.org/10.5772/61103

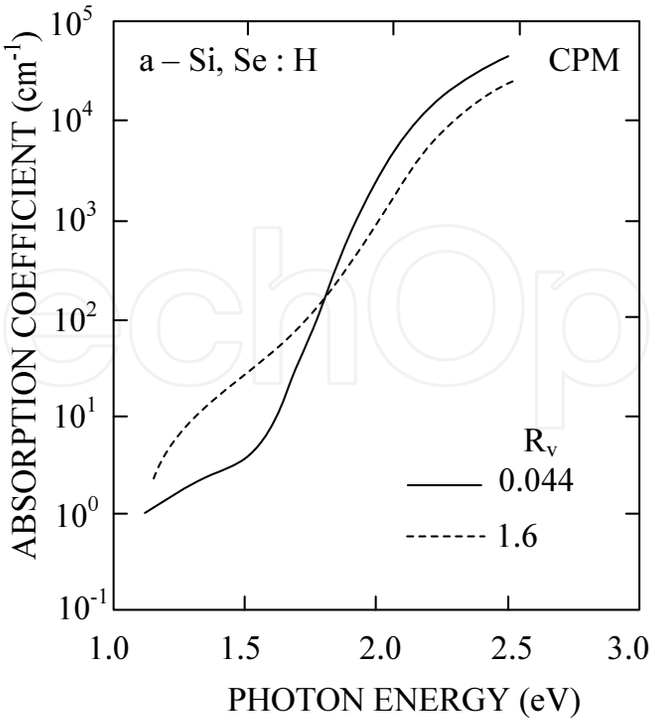

Figure 9. Absorption coefficient as a function of photon energy for two different compositions (R_v = 0.044 and R_v =1.6) (Ref. 18).

portion of the dangling bond defect density in these alloys may have negative correlation energy [22].

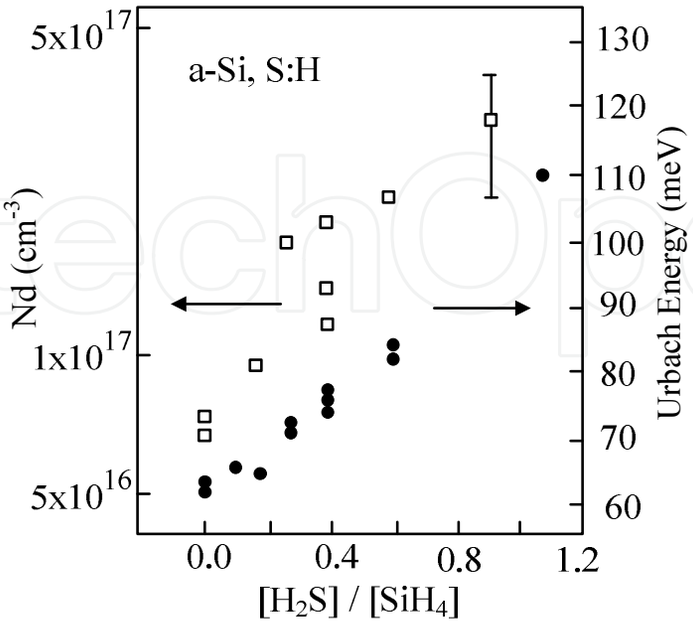

Figure 10. CPM-derived defect density and Urbach energy in a-Si,S:H (Ref. 18).

ii. a-Si,Se:H alloys: The compositional dependence of the Urbach energy E_u and the defect density N_d are shown in Fig. (11). E_u increases rapidly from 60 meV in nonalloyed material (a-Si:H) to 112 meV in selenium-rich samples (R_v = 1.6). This trend suggests a substantial increase in the width of the band tail, as in the case of a-Si,S:H alloys. This observation is consistent with the general trend of increased structural disorder. N_d was obtained from the magnitude of the subgap defect absorption shoulder using the same factor as that used for a-Si:H [44]. Figure (10) shows that N_d increases linearly with R_v from 6×10^{16} cm^{-3} in unalloyed a-Si:H samples to about 2×10^{17} cm^{-3} for R_v = 1.6. The increase in N_d is corroborated preliminary by the ESR measurements of the spin density. It is difficult to compare the spin densities with defect densities obtained from CPM measurements since it is not clear whether the dangling bonds have predominantly positive or negative correlation energies [22].

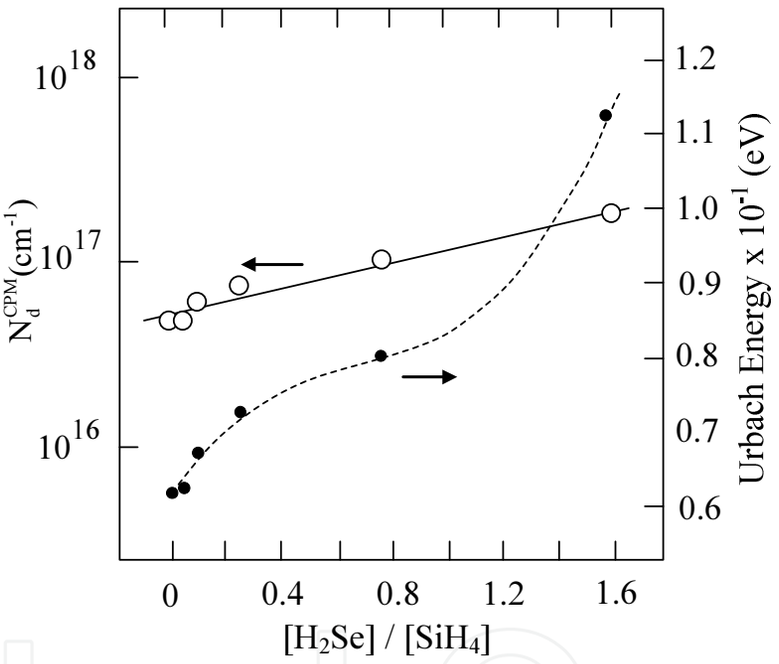

Figure 11. Compositional dependence of the Urbach energy and defect density in a-Si,Se:H alloys (Ref. 17).

3.4. Dark conductivity and photoconductivity

Photoconductivity is a valid probe of the electronic quality of materials. Measurements of the electrical conductivity (σ_d) and photoconductivity (σ_{ph}) for both a-Si,S:H and a-Si,Se:H alloys as a function of the gas volume ratio (R_v) provide a good indication about the effect of defect density in these materials. Figure (12) shows the variation of σ_d and σ_{ph} with composition (R_v) in a-Si,S:H alloys [19]. σ_d decreases monotonically with increasing sulphur content. Room temperature activation energies on the order of 0.95 eV or less are typical for samples containing a high concentration of sulphur (>10 at.%) [19]. For the same range of R_v, the photoconductivity drops by about five orders of magnitude.

http://dx.doi.org/10.5772/61103

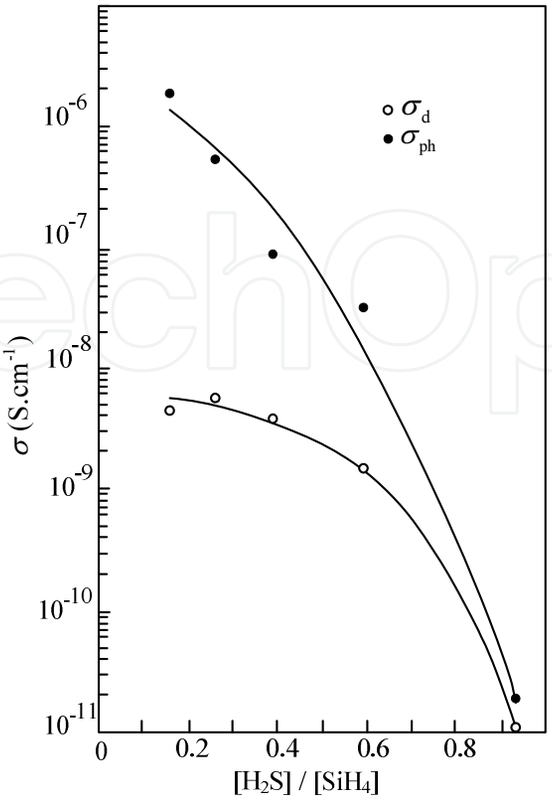

Figure 12. Compositional dependence of dark conductivity (σ_d) and photoconductivity (σ_{ph}) of a-Si_{1-x} S_x alloys. Excitation was performed using a He-Ne laser (10^{15} photon cm^{-2}) (Ref. 15).

Figure (13) shows the variation of σ_d and σ_{ph} for a-Si,Se:H alloys. σ_{ph} was measured with band-pass filtered illumination from a tungsten-halogen lamp providing a uniform carrier generation rate of 10^{21} cm^{-1} s^{-1}. The photoconductivity (σ_{ph}) was found to drop by four orders of magnitude when R_v, and consequently E_{opt}, increases from 1.85 to 2.1 eV. However, the photosensitivity (σ_{ph}/σ_d) remains high, exceeding 10^3 throughout most of the composition range [22].

3.5. Photoluminescence

The photoluminescence (PL) spectra of a-Si,S:H alloy thin films were taken with an excitation energy of 2.41 eV and recorded with a cooled Ge diode [22]. Figure (14) summarizes the variation of integrated intensity (I_{ph}), the full width at half maximum (FWHM) and the photoluminescence peak position as a function of E_{opt}. The PL efficiency η_{PL} drops by a factor of 1/30 when going from unalloyed film to an alloy grown at R_v = 0.93. The PL peak position remains approximately constant at 1.3 eV for all compositions. The FWHM increases from approximately 0.28 eV in the unalloyed material to about 0.60 eV for the samples with the highest sulphur content. These data are evidence of an increase in the width of the band tails with alloying, and in good agreement with earlier results on the variation of Urbach energy with composition. The drop of η_{PL} is a direct consequence of the increase of nonradiative recombination centers as demonstrated by the ESR measurements of N_s [22].

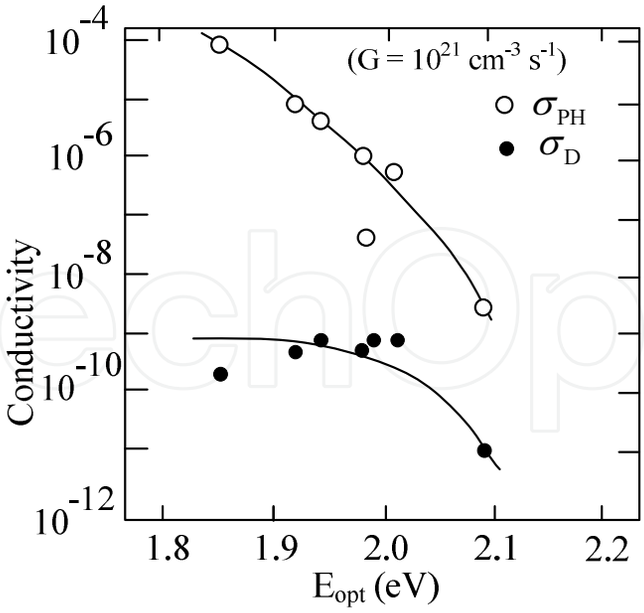

Figure 13. Dark conductivity (σ_d) and photoconductivity (σ_{ph}) versus E_{opt} for a-S,Se:H samples prepared at various compositions (Ref. 17).

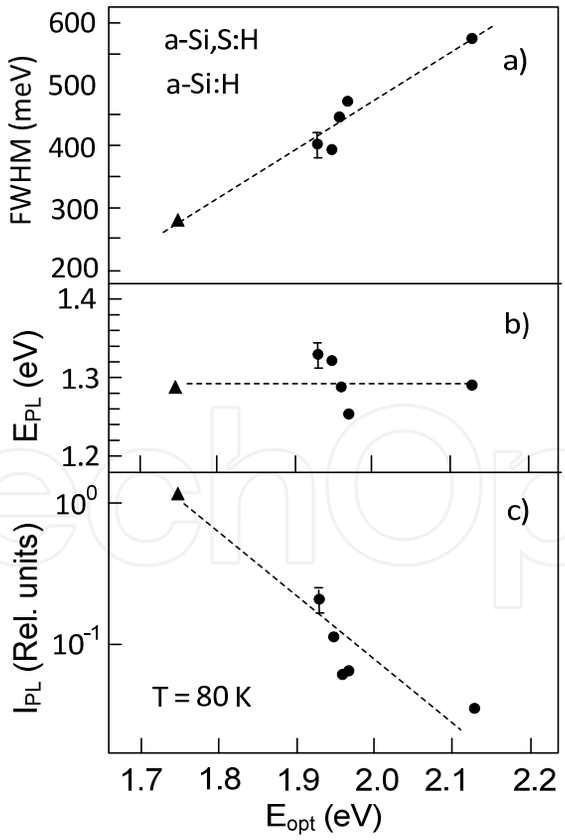

Figure 14. PL peak energy, FWHM, and intensity for various composition of a-Si,S:H alloys (Ref. 18).

http://dx.doi.org/10.5772/61103

4. Conclusions

This work is a review of the structural, spectroscopic, optical, and electronic properties of hydrogenated amorphous silicon-chalcogen alloys. The two alloys considered in this work are a-Si,S:H and a-Si,Se:H. It has been shown that thin films of these materials can be prepared over a relatively wide range of compositions by the glow discharge decomposition of a mixture of either H_2S or H_2Se and SiH_4 gas. Infrared transmission spectroscopy has been employed to probe the bonding structure of these alloys. In a-Si,S:H three sulphur-induced bands at 480, 710, and 760 cm^{-1} have been identified, and several conclusions on their origin have been discussed. The existence of the 480 cm^{-1} band, attributed to Si-S bonds, proves that sulphur can be bonded to the silicon matrix. A shift of the SiH and SiH_2 stretching frequencies have been observed, indicating the presence of significant levels of SiH_xS_y configurations in a-Si,S:H alloys. In a-S-,Se:H, infrared spectroscopy measurements reveal the existence of a spectral feature at 390 cm^{-1}, ascribed to Si-Se bonds. It has been also observed that the SiH and SiH_2 stretching mode frequencies shift to higher wave numbers with increasing selenium content, and thus provide evidence for the presence of significant levels of $(Si)_xSe_{3-x}SiH$ and $(Si)ySe_{2-y}$ SiH_2 configurations in a-Si,Se:H alloys.

Optical absorption measurements carried out on a-Si,S:H and a-Si,Se:H alloys reveal that incorporation of chalcogen atoms in the gaseous phase increases the band gap of these materials. Subgap absorption measurements were carried out to investigate the distribution of defect states in the band gap. It was found that there is a systematic increase in Urbach energy and defect density as the concentration of chalcogen atoms in the gaseous phase increases, and thus indicate a substantial increase in the width of the band tails.

Photoconductivity measurements on these alloys show a decrease in σ_{ph} with increasing E_{opt}. However, the photosensitivity (σ_{ph}/σ_d) remains high.

Photoluminescence measurements show that incorporation of chalcogen atoms in a-Si:H causes a drop in PL efficiency and an increase in the FWHM, again providing further evidence of an increase in the width of the band tail with alloying.

Author details

Shawqi Al Dallal*

Address all correspondence to: shaldallal@gmail.com

College of Graduate Studies and Research, Ahlia University, Manama, Bahrain

References

[1] J. Chevallier, S. Kalem, S. Al Dallal, and J. Bourneix, *Journal of Non-Crystalline Solids*, 51, p. 277 (1982).

[2] S. Girson, F. Briones, and S. L. Vicent, *Philosophical Magazine*, 56, p. 449 (1987).

[3] A. D. Stewart, and D. I. Jones, *Philosophical Magazine*, B57, p. 431 (1988).

[4] P. Harper, and B. Wherrett, *Nonlinear Optics*, Academic Press, New York (1977).

[5] F. Z. Henari, *Optics Communications*, 281, p. 5894 (2008).

[6] G.M. Ferreira, Chi Chen, R.J. Koval, J.M. Pearce, R. W. Collins, and C. R. Wronski, *Journal of Non-Crystalline Solids*, 338–340, p. 694 (2004).

[7] Ken Zweibel, *Solar Energy Materials & Solar Cells*, 63(4), p. 375, (2000).

[8] J. M. Pearce, N. Podraza, R. W Collins, M. M. Al-Jassim, Jones, K. M., J Deng, and C. R Wronski, *Journal of Applied Physics,* 101 (11): 114301-7 (2007).

[9] R. J. Koval, Chi Chen, G. M. Ferreira, A. S. Ferlauto, J. M. Pearce, P. I. Rovira, C. R. Wronski, and R. W. Collins, *Materials Research Society Symposium Proceedings.* 715, A6.1,(2002).

[10] J. Bullot and M. P. Schmidit, *Physica Status Solidi (b)*, 143(2), fmi–fmi, 345–806, K95–K166 (1987).

[11] A. Carbone, F. Demichelis, G. Kaniadakis, G. Della Mea, F. Freire, and P. Rava. *Journal of Materials Research*, 5(12), pp. 2877–2881(1990).

[12] B. Racine, A. C. Ferrari, N. A. Morrison, I. Hutchings, W. I. Milne, and J. Robertson, *Journal of Applied Physics*, 90, 10, p. 15 (2001).

[13] R. Martins, J. Figueiredo, V. Silva, H. Aguas, F. Soares, A. Marques, I. Ferreira, and E. Fortunato, *Journal of Non-Crystalline Solids*, 299, p. 1283, (2002).

[14] E. Fortunato, L. Pereira, H. Aguas, I. Ferreira, and R. Martins, *Proceedings of IEEE*, 93, p. 1281, (2005).

[15] R. Martins, L. Raniero, L. Pereira, D. Costa, H. Aguas, S. Pereira, L. Silva, A. Gonçalves, I. Ferreira, and E. Fortunato, *Philosophical Magazine*, 89, 28–30, pp. 2699–2721, (2009).

[16] R. Martins, H. Aguas, I. Ferreira, E. Fortunato, S. Lebib, and P. R. I Cabarrocas, *Chemical Vapor Deposition*, 9, 6, pp. 333–337, (2003).

[17] S. Al Dallal, S. Al Alawi, and Mahmood Hammam, *Journal of Non-Crystalline Solids*, 356, pp. 2323–2326, (2010).

[18] S. Al-Dallal, S. M. Al-Alawi, and S. Aljishi, *Proceedings of the 6th International Symposium on Advanced Materials*, (1999).

[19] S. Al-Dallal, M. Hammam, and S. M. Al-Alawi, *Philosophical Magazine B*, 63, p. 839 (1991).

[20] S. Al-Dallal, M. Hammam, and S. Al-Alawi, *Journal of Non-Crystalline Solids*, 114, p. 789 (1989).

[21] S. Al-Dallal, S. Aljishi, M. Hammam, S. M. Al-Alawi, M. Stutzmann, Shu Jin, T. Muschik, and R. Schwarz. *Journal of Applied Physics* 70 (9), p. 4926, (1991).

[22] S. Aljishi, S. Al-Dallal, S. M. Al-Alawi, M. Hammam, H. S. Al-Alawi, Stutzmann, S. Jin, T. Muschik, and R. Schwarz, *Solar Energy Materials,* 23, p. 334 (1991).

[23] S. Al-Dallal, M. Hammam, S. M. Al-Alawi and S. Aljishi, *Thin Solid Films*, 205, p. 89, (1991).

[24] S. Al-Dallal, F.Z. Henari, S. M. Al-Alawi, S. R. Arekat, and H. Manaa, *Journal of Non-Crystalline Solids*, 345–346, p. 302 (2004).

[25] S. Al-Dallal, S. Aljishi, M. Hammam, S. M. Al-Alawi, and R.Schwarz, *Proceedings of the International Conference on Condensed Matter Physics (ICCMPA)*, April 13–16, p. 331, (1992).

[26] G. Lucovsky, R.J. Nemanich, and J.C. Knights, *Physical Review B*, 19, p. 2064 (1979).

[27] M. H. Brodsky, and M. Cardona, and J. J. Cuomo, *Physical Review B*, 16, p. 3556 (1977).

[28] E. C. Freeman, and W. Paul, *Physical Review B*, 18, p. 4288 (1978).

[29] H. Shanks, C. J. Fang, L. Ley, M. Cardona, F. J Demond, and S. Kalbitzer, *Physica Status Solidi (b)*, 100, 43 (1980).

[30] G. Lucovsky, *Solid State Communications*, 29, 571(1979).

[31] Sanderson, R. T., *Chemical Bonds and Bond Energy*. San Diego: Academic Press, p. 41 (1976).

[32] C. J. Fang, L. Ley, H. R. Shanks, K. J. Gruntz, and M. Cardona, *Physical Review B*. 22, p. 6140 (1980).

[33] R.Tsu, M. Izu, S. R Ovshinsky, and F. H, Pollak, *Solid State Communications*, 36, p. 817 (1980).

[34] J. Chevallier, S. Kalem, S. Al Dallal, and J. Bourneix, *Journal of Non-Crystalline Solids*, 51, p. 277 (1982).

[35] L. J. Bellamy, *The Infrared Spectra of Complex Molecules*, vol. 1. London: Chapman & Hall, p. 394 (1975).

[36] S. Aljishi, M. Stutzmann, S. Jin, C. Herrero, S. Al Dallal, M. Hammam, and S. M. Al-Alawi, Proc. 13th ICALS Conf., *Journal of Non-Crystalline Solids* (1989).

[37] E. A. Ebsworth, R. Taylor, and L. A. Woodward, *Transactions of the Faraday Society*, 55, p. 211 (1959).

[38] M. Tenhover, R. S. Henderson, D. Lukco, M. A. Hazle, and R. K. Grasselli, *Solid State Communications*, 51, 455 (1984).

[39] K. M. Guggenheimer, *Proceedings of the Physical Society*, 58, p. 456 (1946).

[40] D. R. Herschback, and V. W. Laurie, *Journal of Chemical Physics*, 35, p. 458 (1961).

[41] R. M. Atkins, and P. L. Timms, *Spectrochemica Acta*, 33A, p. 853 (1977).

[42] N. Saito, T. Yamada, Yamagushi, I. Nakaaki, and N. Tanaka, *Philosophical Magazine* B52 (5) (1985).

[43] S. Al Dallal, S. Al Alawi, and M. Hammam, *Journal of Non-Crystalline Solids*, 356, pp. 2323–2326 (2010).

[44] Z. E. Smith, V. Chu, SK. Shepard, S. Aljishi, J. Kolodzey, D. Slobodin, T. L. Chu, and S. Wagner, Physics Letters, 50, p. 1521 (1987).